

Conformational Analysis of Chain Molecules in Liquid Crystalline Phases by a Rotational Isomeric State Scheme with Maximum Entropy Method II. ²H NMR Quadrupolar Splittings from *n*-Decane and 1,6-Dimethoxyhexane Dissolved in 4'-Methoxybenzylidene-4-*n*-butylaniline

Yuji SASANUMA[†]

*Department of Materials Technology, Faculty of Engineering, Chiba University,
1-33 Yayoi-cho, Inage-ku, Chiba 263-8522, Japan*

(Received May 17, 2000; Accepted June 21, 2000)

ABSTRACT: By a rotational isomeric state scheme with the maximum entropy method [Y. Sasanuma, *Polym. J.*, **10**, 883 (2000)], conformational analysis of *n*-decane and 1,6-dimethoxyhexane dissolved in a nematic liquid crystal 4'-methoxybenzylidene-4-*n*-butylaniline (MBBA) was carried out based on ²H NMR quadrupolar splittings from perdeuterated compounds at different temperatures and concentrations. All experimental observations were exactly reproduced by simulation. In MBBA, solute chains are more rigid and extended than in the free state. 1,6-Dimethoxyhexane was found to keep its intrinsic conformational characteristics even in nematic solvent; the *gauche* fraction of the OC-CC bond was comparatively large. Orientational order parameters $\langle S_{ZZ} \rangle$ of the two solutes, plotted against reduced temperature, formed a master curve and were linearly correlated to $\langle S_{ZZ} \rangle$ of MBBA within the observed range.

KEY WORDS *n*-Decane / 1,6-Dimethoxyhexane / 4'-Methoxybenzylidene-4-*n*-butylaniline (MBBA) / Orientational Order Parameter / ²H NMR Quadrupolar Splitting / Rotational Isomeric State Scheme / Maximum Entropy Method /

In the preceding paper¹ (paper I) a rotational isomeric state (RIS) scheme with the maximum entropy (Max-Ent) method was applied to analysis of ¹H-¹H dipolar couplings from *n*-alkanes dissolved in a nematic solvent Kodak EK11650 *p*-pentylphenyl-2-chloro(4-benzylbenzoyloxy)-benzoate. In this paper the method is extended to analysis of ²H NMR quadrupolar splittings² from perdeuterated *n*-decane and 1,6-dimethoxyhexane (1,6-DMH) in a nematic liquid crystal, 4'-methoxybenzylidene-4-*n*-butylaniline (MBBA, see Figure 1).

The reasons for using these systems are as follows. (1) In the previous simulation for *n*-alkanes,¹ 10–20 ¹H-¹H dipolar couplings could be used. Only five and four deuterium quadrupolar couplings can be observed from *n*-decane and 1,6-DMH, respectively. Thus it is meaningful to check the applicability of the modified RIS scheme to conformational analysis based on such a limited number of observations. (2) 1,6-Dimethoxyhexane has the same number of skeletal bonds as *n*-decane but exhibits quite different conformational characteristics in the free state. From *ab initio* molecular orbital (MO) calculations at the second-order Møller-Plesset (MP2) level using the 6-311+G* basis set and geometries optimized by the Hartree-Fock (HF) calculation with the 6-311+G* basis set (MP2/6-311+G*/HF/6-311+G*), first-order interaction energies (E_p , $E_{\sigma 1}$, $E_{\sigma 2}$, and $E_{\sigma 3}$) for bonds 2, 3, 4, and 5 of 1,6-DMH in the gas phase were estimated as 1.29, -0.46, 0.67, and 0.58 kcal mol⁻¹ respectively, and second-order ω_1 and ω_2 interaction energies as 0.20 and 1.39 kcal mol⁻¹ respectively³ (for assignments of statistical weights, see Figure 2). Thus it is interesting to investigate differences in conformation and orientation between *n*-decane and 1,6-DMH dis-

solved in the same nematic solvent. (3) Since order parameters of the solvent MBBA were evaluated from ²H NMR quadrupolar splitting and ²H-¹H dipolar coupling of partially deuterated mesogen,² the orientation of solutes may be expressed as a function of that of MBBA as well as temperature and concentration. (4) ²H NMR measurements were carried out for dilute solutions, of which solute concentration ranges from *ca.* 0.5 to 6.0 mol%. The results here may be comparable to thermodynamic estimation of the solute rigidity (flexibility) from phase behavior.^{2,4,5}

THEORETICAL BASIS

Deuterium quadrupolar splitting $\Delta\nu_i$ from the C-D bond at the *i*th atomic group is given by

$$\Delta\nu_i = \sum_k^K f_k \Delta\nu_{i,k} \quad (1)$$

where K is the number of conformers, and f_k fraction of a conformer k . The quadrupolar splitting $\Delta\nu_{i,k}$ from the conformer k is expressed as⁶

$$\Delta\nu_{i,k} = \frac{3}{2} \frac{e^2qQ}{h} \left[S_{ZZ_k} \frac{3\cos^2\theta_{Z,i,k} - 1}{2} + (S_{XX_k} - S_{YY_k}) \times \frac{\cos^2\theta_{X,i,k} - \cos^2\theta_{Y,i,k}}{2} \right] \quad (2)$$

where e^2qQ/h is the quadrupolar coupling constant (=163 kHz),⁷ X , Y , and Z axes are the principal axes of the order matrix, S_{ZZ_k} , $S_{XX_k} - S_{YY_k}$ are order parameters of the conformer, and, *e.g.*, $\theta_{X,i,k}$ is the angle between the X axis and C- i -D bond. As in paper I, the principal axes of

[†] To whom correspondence should be addressed (Phone: 043-290-3394, Fax: 043-290-3395, E-mail: sasanuma@planet.tc.chiba-u.ac.jp).

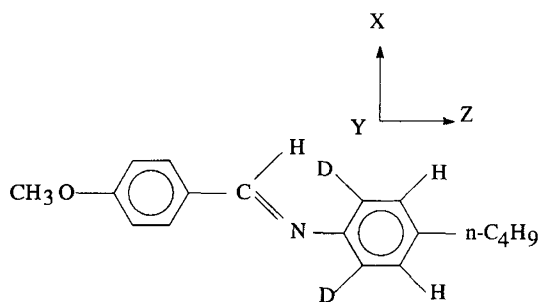


Figure 1. 4'-Methoxybenzylidene-4-*n*-butylaniline (MBBA), nematic solvent used in this study. The molecular axes, *X*, *Y*, and *Z*, are defined with respect to the mesogenic core. Orientational order parameters were determined from ^2H NMR quadrupolar splitting and ^2H - ^1H dipolar coupling of 4-methoxybenzylidene-4-*n*-butylaniline- $d_{2,2,6}$.

inertia are used as *X*, *Y*, and *Z* axes, and the order parameters are calculated from eqs 6 and 7 of paper I.

Statistical weight matrixes of *n*-alkanes (eqs 4 and 5 of paper I) have been applied to *n*-decane. For 1,6-DMH in a nematic field, if up to second-order interactions are considered, statistical weight matrixes U_{ns} (*n*:bond number) may be given as

$$U_2 = \begin{pmatrix} 1 & \rho' & \rho' \\ 0 & 0 & 0 \\ 0 & 0 & 0 \end{pmatrix} \quad (3)$$

$$U_3 = \begin{pmatrix} 1 & \sigma'_1 & \sigma'_1 \\ 1 & \sigma'_1 & 0 \\ 1 & 0 & \sigma'_1 \end{pmatrix} \quad (4)$$

$$U_4 = \begin{pmatrix} 1 & \sigma'_2 & \sigma'_2 \\ 1 & \sigma'_2 & \sigma'_2 \omega'_1 \\ 1 & \sigma'_2 \omega'_1 & \sigma'_2 \end{pmatrix} \quad (5)$$

$$U_5 = \begin{pmatrix} 1 & \sigma'_3 & \sigma'_3 \\ 1 & \sigma'_3 & 0 \\ 1 & 0 & \sigma'_3 \end{pmatrix} \quad (6)$$

$$U_6 = \begin{pmatrix} 1 & \sigma'_2 & \sigma'_2 \\ 1 & \sigma'_2 & 0 \\ 1 & 0 & \sigma'_2 \end{pmatrix} \quad (7)$$

$$U_7 = \begin{pmatrix} 1 & \sigma'_1 & \sigma'_1 \\ 1 & \sigma'_1 & \sigma'_1 \omega'_1 \\ 1 & \sigma'_1 \omega'_1 & \sigma'_1 \end{pmatrix} \quad (8)$$

and

$$U_8 = \begin{pmatrix} 1 & \rho' & \rho' \\ 1 & \rho' & 0 \\ 1 & 0 & \rho' \end{pmatrix} \quad (9)$$

Here, the rows and columns are indexed to rotational states for preceding and current bonds, respectively.⁸ Statistical weight parameters with superscripts of prime include the effects of the nematic field and differ from those for the free state.

For all *n*-alkanes in paper I, statistical weight parameters ω'_n s were virtually null. This indicates that the hydrocarbonic solutes hardly have $g^\pm g^\mp$ conformational

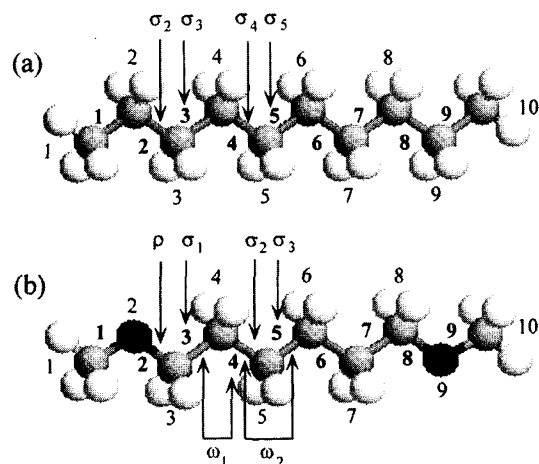


Figure 2. Schematic representation of (a) *n*-decane and (b) 1,6-dimethoxyhexane (1,6-DMH) in all-*trans* conformations. The skeletal bonds and atomic groups (carbon atoms) are numbered, and statistical weight parameters are defined.

sequences (pentane effect⁸) in Kodak EK11650 even at high solute concentration of 30 mol%. Therefore, ω'_n ($n=3, 4,$ and 5) parameters have been assumed null for *n*-decane in MBBA.

For 1,6-DMH, the (2,3) and (3,2) elements of U_3 and U_3 are set to zero, because a severe steric conflict between $\text{C}^1\text{H}_3(\text{C}^{10}\text{H}_3)$ and $\text{C}^5\text{H}_2(\text{C}^6\text{H}_2)$ groups does not allow bonds 2 and 3 (8 and 7) to take $g^\pm g^\mp$ conformations. Here, the superscripts represent carbon numbers (see Figure 2). By geometrical optimization using MO calculation, the $g^+ g^- \text{tttt}$ conformation converged to $g^+ \text{ttttt}$.³ In $g^\pm g^\mp$ conformations for the 4-5 and 5-6 bond pairs, two methylene units, $\text{C}^3\text{H}_2(\text{C}^8\text{H}_2)$ and $\text{C}^7\text{H}_2(\text{C}^4\text{H}_2)$, approach each other, and this is considered equivalent to the pentane effect of *n*-alkanes. The corresponding (2,3) and (3,2) elements of U_5 and U_6 were thus set equal to zero. Previous conformational analysis⁹ of dimethoxy ethers, $\text{CH}_3\text{O}(\text{CH}_2)_y\text{OCH}_3$ ($y=4, 5, 6, 7,$ and 8), showed the presence of intramolecular $(\text{C}-\text{H})\cdots\text{O}$ interactions in $g^\pm g^\mp$ conformations for succeeding OC-CC and CC-CC bonds and represented by statistical weight ω_1 . The sign and magnitude of the second-order interaction energy E_{ω_1} depended on the number of methylene units between two oxygen atoms. By the *ab initio* MO calculations at MP2/6-31+G*//HF/6-31G* level, E_{ω_1} of the gaseous dimethoxy ethers ($y=4, 5, 6, 7,$ and 8) were $-0.43, 0.66, 0.24, 0.42,$ and $0.55 \text{ kcal mol}^{-1}$, respectively. MO calculation at the MP2/6-311+G*//HF/6-311+G* level yielded E_{ω_1} of $0.20 \text{ kcal mol}^{-1}$ for gaseous 1,6-DMH. Therefore, the parameter ω'_1 was treated as an adjustable parameter.

In simulation, almost the same procedure as in paper I was taken. For *n*-decane, five experimental deuterium quadrupolar splittings were simulated using five variables $C(T,c), \sigma'_2, \sigma'_3, \sigma'_4,$ and σ'_5 , while, for 1,6-DMH, four experimental data were reproduced with six parameters $C(T,c), \rho', \sigma'_1, \sigma'_2, \sigma'_3,$ and ω'_1 . Even when the parameters outnumber the data, the MaxEnt method derives the most probable conclusion. The conformer probability of the solute must satisfy the reproducibility of experimental observation. As the initial model m_{ks} in

Table I. Geometrical parameters of 1,6-DMH^a

Bond length/Å	
C-D	1.087
C-C	1.525
C-O	1.392
Bond angle/degree	
∠DCD of methyl group	108.87
∠DCO	110.07
∠COC	114.51
∠OCC	109.09
∠CCC	112.85
∠DCC	109.32
Dihedral angle for <i>gauche</i> state/degree	
bond 2	±99.66
bond 3	±116.12
bond 4	±114.02
bond 5	±114.87
Van der Waals radius/Å	
D	1.20
C	1.70
O	1.52

^a Determined by geometrical optimization using *ab initio* molecular orbital calculations at the HF/6-311+G* level.

eq 11 of paper I, conformer populations in the free state were used. As the conformational energies corresponding to the free state, $E_\sigma=0.5$ and $E_\omega=2.0$ kcal mol⁻¹ were used for *n*-decane,¹⁰ and $E_\rho=1.29$, $E_{\sigma_1}=-0.46$, $E_{\sigma_2}=0.67$, $E_{\sigma_3}=0.58$, $E_{\omega_1}=0.20$, and $E_{\omega_2}=1.39$ kcal mol⁻¹ (the *ab initio* MO calculations at the MP2/6-311+G*/HF/6-311+G* level for the gas phase) were assumed for 1,6-DMH.³

Reproducibility of experiment was checked by the χ^2 parameter (eq 10, paper I) between calculated and observed $\Delta\nu_i$.¹¹

RESULTS AND DISCUSSION

Analysis

For *n*-decane, the geometrical parameters listed in Table I of paper I were employed. For 1,6-DMH, geometries optimized by MO calculations at the HF/6-311+G* level were used (Table I of this paper).³ ²H NMR measurements were carried out for MBBA solutions containing *n*-decane of 0.498, 1.99, 3.99, and 6.07 mol% or 1,6-DMH of 0.505, 2.01, 4.01, and 6.13 mol%. The experimental details were already reported.² Here analysis of ²H NMR data obtained from the most dilute solutions (0.498 mol% for *n*-decane and 0.505 mol% for 1,6-DMH) at 27°C was conducted, and the results are described in detail.

In Table II calculated ²H NMR quadrupolar splittings are compared with corresponding observations. In the table are ²H-²H dipolar couplings between deuterons attached to the same carbon atom. Dipolar couplings were concomitantly evaluated from optimal parameters in Table II. For *n*-decane and 1,6-DMH, the calculations reproduced the observed quadrupolar splittings exactly within the significant figures. ²H-²H dipolar couplings also show satisfactory agreement with experiment.

In Table III optimal variables are listed. ω'_1 of 1,6-DMH was determined to be 1.35, *i.e.*, larger than unity, possibly due to weak (C-H)⋯O attraction between the O² (O⁹) atom and C⁶H₂(C⁵H₂) group of 1,6-DMH dis-

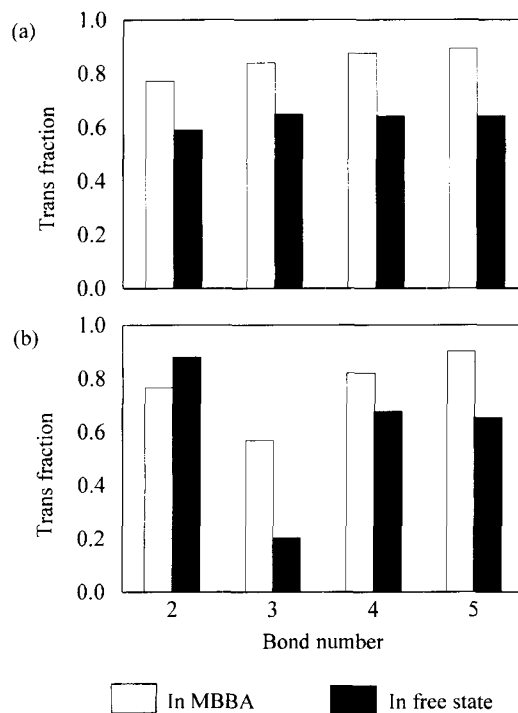


Figure 3. Fractions of the *trans* conformation in skeletal bonds of (a) *n*-decane and (b) 1,6-DMH. For bond numbers, see Figure 2.

solved in MBBA.⁹

Conformations of Solutes in Dilute Solutions

Using statistical weight parameters in Table III, we calculate the *trans* fraction $p_{t;n}$ of the *n*th bond from⁸

$$p_{t;n} = \frac{\mathbf{J}^* [U_2 \dots U_{n-1} U_n(t) U_{n+1} \dots U_{N-1}] \mathbf{J}}{\mathbf{J}^* \left[\prod_{n=2}^{N-1} U_n \right] \mathbf{J}} \quad (5)$$

where $\mathbf{J}^* = [100]$, \mathbf{J} is the 3×1 column matrix of which elements are unity, and N is the number of skeletal bonds. The $U_n(t)$ matrix can be obtained by filling the columns corresponding to the g^\pm states of U_n with zero.

In Figure 3, *trans* fractions of the skeletal bonds are shown as a histogram and compared with those for the free state. As seen from the figure, *trans* fractions of *n*-decane and 1,6-DMH in MBBA are, in principle, larger than those for the free state. Thus, in MBBA, both molecules are more rigid and extended than in the free state. This is also confirmed from the average distance between the terminal methyl carbons $\langle r \rangle$; $\langle r \rangle$ of *n*-decane and 1,6-DMH was estimated as 10.44 (9.26 Å) and 9.62 (8.49 Å) respectively. The values in parentheses represent those in the free state. As in paper I, the *n*-decane molecule dissolved in Kodak EK11650 at a solute concentration of 30 mol% gave rather smaller $\langle r \rangle$ of 9.78 Å.

For *n*-decane, the *trans* fraction increases gradually from the terminal to central bond. 1,6-DMH exhibits more complicated conformational features. Bond 3 prefers the *gauche* conformation to the *trans* one in the free state. This property is somewhat kept in the nematic field. For bonds 4 and 5, *trans* fractions are somewhat enhanced compared with those in the free state.

The *trans* fraction of bond 2 was smaller than that in

Table II. Calculated and observed ^2H NMR quadrupolar splittings and ^2H - ^2H dipolar couplings of *n*-decane and 1,6-DMH

Atomic-group No. ^a	<i>n</i> -decane				1,6-DMH			
	$ \Delta\nu_i ^b$		$ D_{DD,i} ^c$		$ \Delta\nu_i ^b$		$ D_{DD,i} ^c$	
	Calcd	Obsd ^d	Calcd	Obsd ^d	Calcd	Obsd ^d	Calcd	Obsd ^d
1	7.95	7.95	—	—	8.60	8.60	—	—
2	25.93	25.93	60	59	—	—	—	—
3	30.46	30.46	70	70	21.48	21.48	48	—
4	32.97	32.97	75	76	28.31	28.31	59	61
5	33.98	33.98	77	78	29.67	29.67	62	65

^a For atomic-group numbers, see Figure 2. ^b In kHz. ^c In Hz. ^d At 27°C and 0.498 mol% (*n*-decane) or 0.505 mol% (1,6-DMH).

Table III. Optimal parameters ^a

<i>C</i> (<i>T</i> , <i>c</i>)	Bond no. ^b		<i>n</i> -Decane	1,6-DMH
				0.352
Statistical weight parameter ^b				
First order				
	2	σ'_2	0.162	ρ' 0.200
	3	σ'_3	0.117	σ'_1 0.431
	4	σ'_4	0.083	σ'_2 0.108
	5	σ'_5	0.069	σ'_3 0.066
Second order				
	3,4	—	—	ω'_i 1.35

^a Simulation was carried out for ^2H NMR quadrupolar splittings at 27°C and solute concentration of 0.498 mol% (*n*-decane) or 0.505 mol% (1,6-DMH). ^b For bond numbers and assignments of statistical weight parameters, see Figure 2.

the free state. This may be explained as follows. In our previous studies on polyethers,^{12–14} first-order interaction energy for the CO–CC bond of dimethoxy ethers depended on solvent; Conformational energy decreased monotonously with increasing dielectric constant of solvent. E_σ (corresponding to E_σ of interest here) of 1,2-dimethoxypropane was suggested to range from 1.52 kcal mol⁻¹ (in the gas phase, dielectric constant $\epsilon=1.0$) to 1.26 kcal mol⁻¹ (in dimethyl sulfoxide, $\epsilon=45.0$). *Trans* fractions for the free state of 1,6-DMH were calculated from conformational energies estimated for the gas phase. Thus E_p (1.29 kcal mol⁻¹) would be somewhat overestimated for 1,6-DMH surrounded by MBBA molecules. Dielectric constants of MBBA are $\epsilon_{\parallel}=4.7$ (parallel to the nematic axis) and $\epsilon_{\perp}=5.4$ (normal).¹⁵ Conformational energy of the *gauche* state around the OC–CC bond has a comparatively large tolerance. *Ab initio* MO calculations at the MP2/6-31+G*//HF/6-31G* level gave E_p of 0.83 to 1.41 kcal mol⁻¹ for $\text{CH}_3\text{O}(\text{CH}_2)_y\text{OCH}_3$ ($y=4-8$). To sum up, it can be stated that the solute chains keep inherent conformational preference even in the nematic field but have larger *trans* fractions and hence are more anisotropic than in the free state.

In Table IV order parameters of solutes, estimated from eqs 14 and 15 of paper I, are compared with those of solvent MBBA. The solutions were prepared so that solute concentrations would be equal to 0.5 mol%. The order parameters of MBBA were determined using ^2H NMR quadrupolar splitting and ^2H - ^1H dipolar coupling from partially deuterated mesogen, as shown in Figure 1. From $\langle S_{ZZ} \rangle$ in Table IV, 1,6-DMH more disturbs the orientational order of MBBA than *n*-decane. This is consistent with the phase behavior of the dilute solutions.²

Table IV. Orientational order parameters of solutes (*n*-decane and 1,6-DMH) and solvent (MBBA) ^a

	System			
	<i>n</i> -Decane ^b + MBBA ^c		1,6-DMH ^d + MBBA ^e	
	$\langle S_{ZZ} \rangle$	0.294	0.522	0.270
$\langle S_{XX} - S_{YY} \rangle$	0.019	0.017	0.017	0.020

^a At 27°C. Solutions containing either perdeuterated solute or partially deuterated solvent were used. Solute concentrations were ^b 0.498 mol%; ^c 0.504 mol%; ^d 0.505 mol%; and ^e 0.473 mol%.

The ability of the solute to destabilize the nematic phase can be represented by slopes of two boundary lines in the phase diagram of reduced temperature ($T^* = T/T_{NI}$, T_{NI} : the nematic-to-isotropic transition temperature of pure MBBA) vs. molar fraction of solute.^{4,5} At infinite dilution of the *n*-decane + MBBA system, the slope β_N^∞ of the boundary line (T_N^* point) where the isotropic phase appears on heating and the slope β_I^∞ of the boundary line (the T_I^* point) where the nematic phase completely disappears on heating were 0.597 and 0.561, respectively.^{4,5} The 1,6-DMH + MBBA system gave $\beta_N^\infty = 0.899$ and $\beta_I^\infty = 0.820$.² Experimental β_N^∞ of globular solutes range from 0.56 to 1.7, while those of *n*-alkanes are known to fall between 0.53 and 0.63.^{4,5}

Orientational Orders of Solutes and Solvent

In Figure 4 orientational order parameters of solutes at different concentrations are plotted as function of temperature. A convex curve of $\langle S_{ZZ} \rangle$ shifts to lower temperature with increase in concentration. As expected, 1,6-DMH exhibits larger shift than *n*-decane.

In Figure 5, $\langle S_{ZZ} \rangle$ of the solute and solvent, obtained at different concentrations, are shown as function of reduced temperature T/T_N . Both order parameters form individual master curves irrespective of solute. In the vicinity of the T_N^* point, the solute and solvent have $\langle S_{ZZ} \rangle$ of 0.14 and 0.29, respectively. The latter is much smaller than predicted by Maier and Saupe (0.429).¹⁶ In Figure 6, the correlation between $\langle S_{ZZ} \rangle$ of the solute and solvent is shown. The data points are a little scattered but show a linear relationship expressed as $\langle S_{ZZ} \rangle_{\text{solute}} = 0.581 \langle S_{ZZ} \rangle_{\text{MBBA}} - 0.023$ within the observed range. The correlation coefficient was 0.967.

CONCLUSIONS

The RIS scheme with the MaxEnt method was applied to analysis of ^2H NMR quadrupolar splittings observed from perdeuterated *n*-decane and 1,6-DMH dissolved in a nematic solvent MBBA at low solute concentrations and different temperatures. The following results and

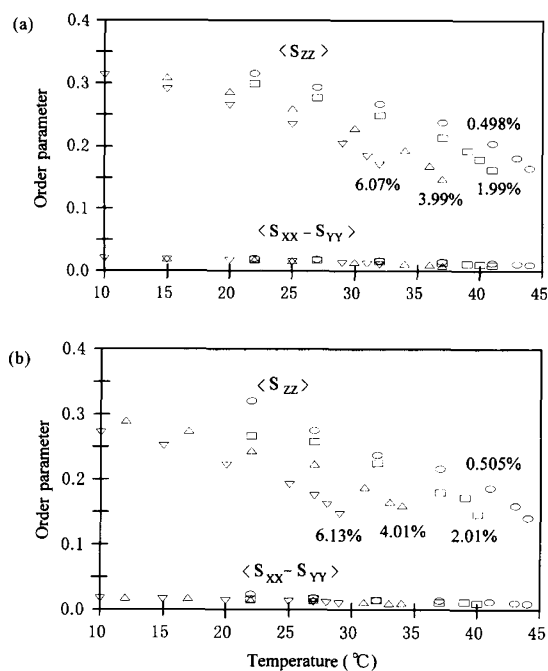


Figure 4. Orientational order parameters, $\langle S_{ZZ} \rangle$ and $\langle S_{XX} - S_{YY} \rangle$, of (a) *n*-decane and (b) 1,6-DMH at different solute concentrations (in mol%), expressed as a function of temperature.

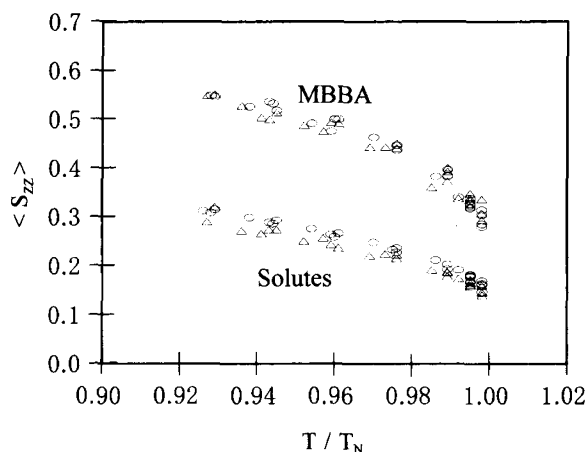


Figure 5. Orientational order parameters of solutes and solvent as function of reduced temperature T/T_N : \circ , *n*-decane+MBBA; \triangle , 1,6-DMH+MBBA.

conclusions were obtained.

(1) By the simulation all experimental data of the deuterium quadrupolar splitting were reproduced exactly within significant figures, and ^2H - ^2H dipolar couplings calculated with optimal parameters were in satisfactory agreement with observation.

(2) In MBBA, C-C bonds of *n*-decane had larger *trans* fraction, and hence the molecule was more rigid and extended than in the free state. Even in the nematic field, 1,6-DMH keeps its intrinsic conformational preference especially in the OC-CC bond. The 1,6-DMH molecule was less anisotropic and more destructive to the nematic order than *n*-decane. These results are consistent with the phase behavior of dilute solutions.

(3) Order parameters $\langle S_{ZZ} \rangle$ s of the solutes, evaluated from ^2H NMR data at different concentrations, formed a

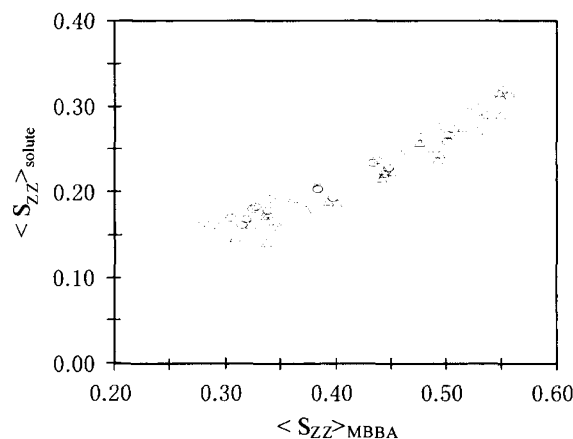


Figure 6. Correlation between $\langle S_{ZZ} \rangle$ of solutes and solvent: \circ , *n*-decane+MBBA; \triangle , 1,6-DMH+MBBA.

master curve against reduced temperature T/T_N . $\langle S_{ZZ} \rangle$ of the solute exhibits a linear correlation with that of the solvent MBBA over a wide temperature range. On heating, the isotropic phase appeared around $\langle S_{ZZ} \rangle_{\text{MBBA}} = 0.29$ ($\langle S_{ZZ} \rangle_{\text{solute}} = 0.14$).

In the preceding¹ and present papers the RIS-MaxEnt scheme was shown applicable to analysis of ^1H - ^1H dipolar couplings observed from *n*-alkanes and ^2H NMR quadrupolar splittings from *n*-decane and 1,6-DMH and provides detailed information on conformations and orientation.

Acknowledgments. This work was supported in part by Grant-in-Aid for Scientific Research (C) (No. 11650920) of Japan Society for the Promotion of Science.

REFERENCES

1. Y. Sasanuma, *Polym. J.*, **10**, 883, (2000).
2. Y. Sasanuma, *J. Phys. II France*, **3**, 1759 (1993).
3. Y. Sasanuma, *J. Phys. II France*, **7**, 305 (1997).
4. D. E. Martire, in "The Molecular Physics of Liquid Crystals", G. R. Luckhurst and G. W. Gray, Ed., Academic Press, New York, N.Y., 1979, Chapter 10.
5. B. Kronberg, D. F. Gilson, and D. Patterson, *J. Chem. Soc., Faraday Trans. 2*, **72**, 1673 (1976).
6. J. W. Emsley, Ed., "Nuclear Magnetic Resonance of Liquid Crystals", Reidel, Dordrecht, 1985.
7. M. S. Greenfield, R. L. Vold, and R. R. Vold, *J. Chem. Phys.*, **83**, 1440 (1985).
8. P. J. Flory, "Statistical Mechanics of Chain Molecules", Interscience, New York, N.Y., 1969.
9. R. V. Law and Y. Sasanuma, *J. Chem. Soc., Faraday Trans.*, **92**, 4885 (1996).
10. A. Abe, R. L. Jernigan, and P. J. Flory, *J. Am. Chem. Soc.*, **88**, 631 (1966).
11. For the details, see S. F. Gull and J. Skilling, "Quantified Maximum Entropy MemSys5 User's Manual", Maximum Entropy Data Consultants Ltd., Cambridge, 1991.
12. Y. Sasanuma, *J. Phys. Chem.*, **98**, 13486 (1994).
13. Y. Sasanuma, *Macromolecules*, **28**, 8629 (1995).
14. R. V. Law and Y. Sasanuma, *Macromolecules*, **31**, 2335 (1998).
15. P. G. de Gennes and J. Prost, "The Physics of Liquid Crystals", 2nd ed, Oxford, New York, N.Y., 1993, pp 230-232.
16. W. Maier and A. Saupe, *Z. Naturforsch., A: Phys. Sci.*, **14**, 882 (1959); **15**, 287 (1960).